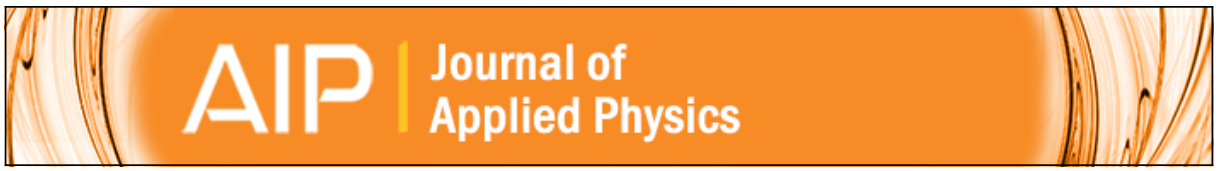

Actuation performances of anisotropic gels

P. Nardinocchi and L. Teresi

Citation: Journal of Applied Physics **120**, 215107 (2016); doi: 10.1063/1.4969046

View online: http://dx.doi.org/10.1063/1.4969046

View Table of Contents: http://scitation.aip.org/content/aip/journal/jap/120/21?ver=pdfcov

Published by the AIP Publishing

Actuation performances of anisotropic gels

P. Nardinocchi[1,a)] and L. Teresi[2,b)]
[1]*Dipartimento di Ingegneria Strutturale e Geotecnica, Sapienza Università di Roma, via Eudossiana 18, 00184 Roma, Italy*
[2]*Dipartimento di Matematica e Fisica, Università Roma Tre, via della Vasca Navale 84, 00146, Roma, Italy*

(Received 2 September 2016; accepted 14 November 2016; published online 7 December 2016)

We investigated the actuation performances of anisotropic gels driven by mechanical and chemical stimuli, in terms of both deformation processes and stroke–curves, and distinguished between the fast response of gels before diffusion starts and the asymptotic response attained at the steady state. We also showed as the range of forces that an anisotropic hydrogel can exert when constrained is especially wide; indeed, changing fiber orientation allows us to induce shear as well as transversely isotropic extensions. *Published by AIP Publishing*. [http://dx.doi.org/10.1063/1.4969046]

I. INTRODUCTION

Soft active materials admit deformations and displacements that can be triggered through a wide range of external stimuli such as electric field, pH, temperature, and solvent absorption.[1–4] The effectiveness of these systems may critically depend on the capability of achieving both prescribed changes in shape and size and on the range of performances in actuator applications, which can involve isotropic or fibrous gels. We recently presented an investigation about fiber reinforced gels, a soft composite material, whose shape changes can be programmed by adjusting both fiber orientation and stiffness, and about the possible shape changes that they realize in free–swelling conditions; we also discussed the role of fibre orientation in determining these shape changes.[5] Moreover, we showed that, by considering geometric composites made of homogeneous layers of fibrous gels, an even larger variety of shapes can be generated starting from a flat strip.[6]

Fibrous or anisotropic gels are at the center of many recent realisation dealing with fibrous soft materials inspired by plant world,[7] natural filtration systems,[8] biomedical materials for cardiovascular medicine,[9] polymer hydrogels with anisotropies in structure and optical properties,[10] as well as theoretical investigations. These different applications exploit the ability of such gels to undergo anisotropic swelling and to show an anisotropic mechanical response; both of these elements characterise the mechanics of fibrous hydrogels.

To the best of our knowledge, the performances of fibrous hydrogels in actuator applications have not been extensively studied.[11] As it is well known, actuators are usually characterized by their force–stroke curves, which deliver critical information when designing an actuator.[12,13] In particular, the range of forces that an anisotropic hydrogel can exert when constrained is especially wide. Indeed, changing fiber orientation in gel cubic elements allows us to induce shear as well as transversely isotropic extensions, under free–swelling conditions.[5] Correspondingly, under appropriate imposed deformations, i.e., boundary constraints, anisotropic gels can exert both tangential and normal forces, depending on fiber orientation. Moreover, due to swelling, such forces decrease from the instantaneous values attained before diffusion starts to the lower values attained at the steady state.[14]

This paper aims to investigate performances of anisotropic gels driven by mechanical and chemical stimuli, in terms of both deformation processes and stroke–curves, and distinguish between the fast response of gels before diffusion starts and the asymptotic response attained at the steady state. We start from a Sec. II devoted to revisit a few results related to isotropic gel actuators. Then, with reference to a thermodynamic model, which can be viewed as the extension of the well–known Flory–Rehner model, a few prototypical anisotropic actuators are investigated, and the corresponding deformation processes and stroke–curves are discussed.

II. BACKGROUND

Our starting point is the multiphysics model presented and discussed in Ref. 15; therein, three different states of a gel body were introduced: a dry state $\mathcal{B}_d$, a swollen and stress–free state $\mathcal{B}_o$, and an actual state $\mathcal{B}_t$ (see cartoon in Figure 1). Then, the constitutive equation for the stress $\mathbf{S}_d$ ($[\mathbf{S}_d] = \text{Pa} = \text{J/m}^3$) at the dry configuration $\mathcal{B}_d$, from now on denoted as dry–reference stress, and that for the chemical potential μ ($[\mu] = \text{J/mol}$) were derived from the classical Flory–Rehner thermodynamic context. The Flory–Rehner model[16,17] for stress diffusion in gels is based on a free energy ψ per unit dry volume, which depends on the deformation gradient $\mathbf{F}_d$ from the initial dry configuration of the polymer gel through an elastic component ψ_e and on the molar solvent concentration c_d per unit dry volume ($[c_d] = \text{mol/m}^3$) through a polymer–solvent mixing energy ψ_m: $\psi = \psi_e + \psi_m$. We include in the definition of the free–energy a volumetric constraint prescribing that changes in volume are only due to solvent absorption or release. In order to account for such a constraint, we relax the Flory–Rehner free energy by adding a term which enforces that constraint and write

a)Electronic mail: paola.nardinocchi@uniroma1.it
b)Electronic mail: teresi@uniroma3.it

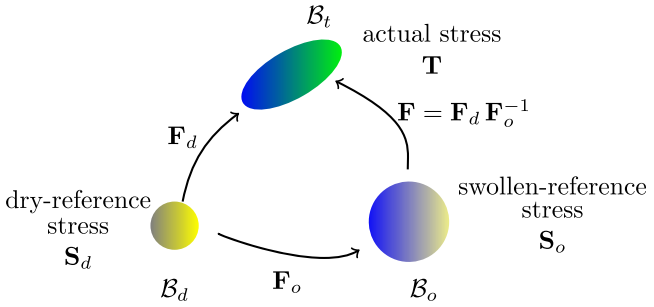

FIG. 1. Given a dry ball $\mathcal{B}_d$, the swollen and stress–free state $\mathcal{B}_o$ only differs for a change in size, whereas the actual state $\mathcal{B}_t$ for a change in size and possibly in shape.

$$\psi_r(\mathbf{F}_d, c_d, p) = \psi_e(\mathbf{F}_d) + \psi_m(c_d) - p(J_d - \hat{J}(c_d)). \quad (2.1)$$

The pressure p represents the reaction to the volumetric constraint, which maintains the volume change due to the displacement equal to the one due to solvent absorption or release

$$J_d = \det \mathbf{F}_d = \hat{J}(c_d) = 1 + \Omega\, c_d, \quad (2.2)$$

being Ω ($[\Omega] = \mathrm{m}^3/\mathrm{mol}$) the solvent molar volume. The function ψ_r is called the Lagrangian function associated with the energy ψ, while p is the Lagrangian multiplier, which measures the sensitivity of the minimum energy to a change in the constraint. Key features of ψ (or ψ_r) are the following: (i) ψ is a density per unit volume of the dry polymer; (ii) the elastic contribution ψ_e hampers swelling; and (iii) the mixing contribution ψ_m favors swelling.

The constitutive equation for the stress $\mathbf{S}_d$ and the chemical potential μ ($[\mu] = \mathrm{J/mol}$) come from thermodynamic issues and prescribe that

$$\mathbf{S}_d = \mathbf{S}_d(\mathbf{F}_d) - p\,\mathbf{F}_d^{\star} \quad \text{and} \quad \mu = \mu(c_d) + p\,\Omega, \quad (2.3)$$

with

$$\mathbf{S}_d(\mathbf{F}_d) = \frac{\partial \psi_e}{\partial \mathbf{F}_d} \quad \text{and} \quad \mu(c_d) = \frac{\partial \psi_m}{\partial c_d}, \quad (2.4)$$

being $\mathbf{F}^{\star} = (\det \mathbf{F})\mathbf{F}^{-T}$. The Flory–Rehner thermodynamic model prescribes a neo-Hookean elastic energy ψ_e

$$\psi_e(\mathbf{F}_d) = \frac{G}{2}(\mathbf{F}_d \cdot \mathbf{F}_d - 3), \quad (2.5)$$

being G the shear modulus of the dry polymer; moreover, it prescribes the following polymer–solvent mixing energy

$$\psi_m(c_d) = \frac{RT}{\Omega}\, h(c_d), \quad (2.6)$$

with

$$h(c_d) = \Omega\, c_d\, \log \frac{\Omega\, c_d}{1 + \Omega\, c_d} + \chi\, \frac{\Omega\, c_d}{1 + \Omega\, c_d}, \quad [h] = 1, \quad (2.7)$$

being R ($[R] = \mathrm{J/(K\,mol)}$), T ($[T] = \mathrm{K}$), and χ the universal gas constant, the temperature, and the Flory parameter, respectively. From $(2.4)_1$ and (2.5), we derive the constitutive equation $\mathbf{S}_d(\mathbf{F}_d)$ for the dry–reference stress; from $(2.4)_2$, (2.6), and (2.7), we derive the constitutive equation $\mu(c_d)$ for the chemical potential. This latter can also be rewritten as a function of J_d by exploiting the volumetric constraint (2.2); with a slight abuse of notation, we write $\mu(c_d) = \mu(J_d)$

$$\mu(J_d) = RT\left(\log \frac{J_d - 1}{J_d} + \frac{1}{J_d} + \frac{\chi}{J_d^2}\right). \quad (2.8)$$

Performances of gels in terms of both deformation processes and stroke–curves driven by mechanical and chemical stimuli can be studied solving a time–dependent stress–diffusion problem based on appropriate balance equations and constitutive prescriptions for $\mathbf{S}_d$, μ, and the solvent flux.[5,15] However, sometimes homogeneous solutions are of interest, corresponding to steady states and/or, on the opposite side, to before–diffusion–starts states. A typical example deals with a gel body embedded into a solvent bath of assigned chemical potential μ_e. In this case, the homogeneous solutions of the problem can be completely determined by data prescribed on the boundary in terms of boundary loads and/or constraints, and μ_e.

The simplest example of such problems is the one with zero boundary loads. In this case, mechanical and chemical balance laws prescribe $\mathbf{S}_d = \mathbf{0}$ and $\mu_e = \mu_o$, that is, the swollen and stress–free state $\mathcal{B}_o$, attained from $\mathcal{B}_d$ with $\mathbf{F}_d = \mathbf{F}_o = \lambda_o \mathbf{I}$, is completely defined by the value μ_o of the bath's chemical potential. The condition of zero stress yields the pressure p

$$G\mathbf{F}_o - p\,\mathbf{F}_o^{\star} = 0 \quad \Rightarrow \quad p = \frac{G}{\lambda_o}. \quad (2.9)$$

By substituting p in the constitutive relation for the chemical potential yields a non linear equation relating μ_o and λ_o[18]

$$\mu(J_o) + \frac{G}{\lambda_o}\,\Omega = \mu_o, \quad \text{with } J_o = \lambda_o^3. \quad (2.10)$$

For large deformation ($1/J_o \to 0$), Equation (2.10) can be approximated, by estimating the leading order term in the Maclaurin asymptotic expansion in $1/J_o$, as[19]

$$\frac{RT}{\Omega}(\chi - 1/2) = \frac{\mu_o}{\Omega} J_o^2 - \frac{G}{\lambda_o} J_o^2. \quad (2.11)$$

In some cases, it may be convenient to use the free-swollen state $\mathcal{B}_o$ as reference configuration; the deformation from $\mathcal{B}_o$ to the actual state $\mathcal{B}_t$ is then described by the deformation gradient $\mathbf{F} = \mathbf{F}_d\,\mathbf{F}_o^{-1}$. The actual (Cauchy) stress $\mathbf{T}$ can then be represented in terms of the dry–reference stress $\mathbf{S}_d$, or of the swollen–reference stress $\mathbf{S}$, defined as the *push–forward* of $\mathbf{S}_d$ and/or the *pull–back* of $\mathbf{T}$

$$\mathbf{S} = \underbrace{\frac{1}{J_o}\mathbf{S}_d\mathbf{F}_o^T}_{push-forward} = \underbrace{\mathbf{T}\mathbf{F}^{\star}}_{pull-back}, \quad \mathbf{T} = \frac{1}{J_d}\mathbf{S}_d\mathbf{F}_d^T. \quad (2.12)$$

Using Equations $(2.3)_1$, $(2.4)_1$, (2.5), and defined $\mathbf{B}_d = \mathbf{F}_d\,\mathbf{F}_d^T$, we have

$$\mathbf{S} = \frac{G}{J_o}\mathbf{F}\mathbf{F}_o\mathbf{F}_o^T - p\mathbf{F}^\star \quad \text{and} \quad \mathbf{T} = \frac{1}{J_d}\,G\,\mathbf{B}_d - p\mathbf{I}. \tag{2.13}$$

The deformation $\mathbf{F}$ can have different characteristics; in the following, we quickly revise two typical problems partially studied in the Literature for isotropic gels.

A. Isotropic gels under step pressure and dilation

Given a free-swollen state $\mathcal{B}_o$, we consider the steady–state $\mathcal{B}_t$ determined by the bath's chemical potential μ_e and by the external pressure p_e. This state is described by the deformation field $\mathbf{F} = \lambda\mathbf{I}$, and we look for homogeneous solutions of the stress–diffusion problem, with boundary conditions

$$\mathbf{T}\,\mathbf{n} = -p_e\,\mathbf{n} \quad \text{and} \quad \mu = \mu_e \quad \text{on } \partial\mathcal{B}_t, \tag{2.14}$$

with $\mathbf{n}$ the unit normal to $\partial\mathcal{B}_t$. Mechanical and chemical balances prescribe the spherical component σ of the stress $\mathbf{T} = \sigma\mathbf{I}$ and the chemical potential within the gel

$$\sigma = -p_e \quad \text{and} \quad \mu = \mu_e \quad \text{in } \mathcal{B}_t. \tag{2.15}$$

Being $\mathbf{F}_o = \lambda_o\mathbf{I}$ and $\mathbf{F} = \lambda\mathbf{I}$, from Equations $(2.3)_1$, $(2.4)_1$, (2.5), and $(2.12)_2$, we obtain σ

$$\sigma = \frac{G}{\lambda_o\,\lambda} - p. \tag{2.16}$$

With this, Equation $(2.15)_1$ relates the (osmotic) pressure p to the external pressure p_e and to the additional deformation λ as

$$p = \frac{G}{\lambda_o\,\lambda} + p_e. \tag{2.17}$$

We focus on the slow response of the gel and assume that solvent migration has reached a steady state. The characteristics of this response are determined by Equation $(2.15)_2$ which, together with Equations $(2.3)_2$ and (2.8), yields an implicit relation between the triplet (p_e, λ, μ_e)

$$\mu(J\,J_o) + \frac{G\,\Omega}{\lambda_o\,\lambda} + p_e\,\Omega = \mu_e, \quad J\,J_o = (\lambda\,\lambda_o)^3. \tag{2.18}$$

Fixed the pair (p_e, μ_e), the stretch λ determines the size of $\mathcal{B}_t$; alternatively, fixed the pair (λ, μ_e) with λ an imposed dilation, p_e determines both the isotropic stress within the body and the intensity of the normal boundary traction (see Equations $(2.14)_1$ and $(2.15)_1$).

We may look for the pressure p_e needed to keep a fixed dilation λ, under different μ_e; in this case, Equation $(2.18)_1$ can be recast as a function delivering p_e in terms of λ and μ_e, with λ_o (or, equivalently, μ_o) as a parameter

$$p_e = p_e(\lambda, \mu_e, \lambda_o) = \frac{1}{\Omega}\left(\mu_e - \mu\left(\lambda^3\,\lambda_o^3\right)\right) - \frac{G}{\lambda_o\,\lambda}. \tag{2.19}$$

Fixed the initial free-swollen conditions determined by μ_o (or, through (2.10), by λ_o), we can have different stroke–curves p_e versus λ, which depend on the new value of μ_e; Figure 2 shows some of these curves for $\mu_o = -10$ J/mol (and correspondingly, $\lambda_o = 2$), and $\mu_e = \mu_o \pm 10$ J/mol, once fixed $\Omega = 6\times10^{-5}$ m^3/mol, $\chi = 0.2$, and $G = 0.1$ MPa. At different values of $\mu_e = -20$, -10, 0 J/mol, pressure–stroke curves intercept the axis $p_e = 0$ at different values of λ which correspond to free–swelling stretches. For $\mu_e = \mu_o = -10$ J/mol, we recover the free-swollen reference state, that is $\lambda = 1$, and $p_e = 0$.

In particular, Equation (2.19) also allows us to discuss the existence of a blocking pressure, that is, a pressure $p_e^\star$ which, depending on the value of μ_e, maintains $\lambda = 1$, that is $\mathcal{B}_t = \mathcal{B}_o$. Equations (2.17) and (2.18) with $\lambda = 1$

$$\frac{G}{\lambda_o} - p = -p_e^\star \quad \text{and} \quad \mu(J_o) + \frac{G\Omega}{\lambda_o} + p_e^\star\Omega = \mu_e, \tag{2.20}$$

characterise the blocking pressure p_e^*

$$p_e^\star = \frac{1}{\Omega}\,(\mu_e - \mu_o). \tag{2.21}$$

As expected, Equation (2.21) gives a null blocking pressure for $\mu_e = \mu_o = -10$ J/mol; increasing (decreasing) μ_e requires a positive (negative) pressure $p_e^\star$ to maintain $\lambda = 1$.

It is worth noting that for large swelling–induced deformations, i.e., $1/J_o \to 0$ and $1/J \to 0$, Equation (2.18) can be approximated as

$$\frac{G}{\lambda_o}\left(\frac{1}{\lambda^6} - \frac{1}{\lambda}\right) = p_e, \tag{2.22}$$

where we set $\mu_o = \mu_e = 0$.

B. Isotropic gels under step traction and extension

We consider a dry-reference cubic gel $\mathcal{B}_d$, whose edges are aligned along the directions of the orthonormal basis $(\mathbf{e}_1, \mathbf{e}_2, \mathbf{e}_3)$ of the three–dimensional vector space $\mathcal{V}$ (see Figure 3, panel a), and its free-swollen state $\mathcal{B}_o$, determined by the value μ_o of the solvent's bath chemical potential (see Figure 3, panel b). The gel may undergo further deformations, determined by a change $\mu_e - \mu_o$ of the solvent bath's

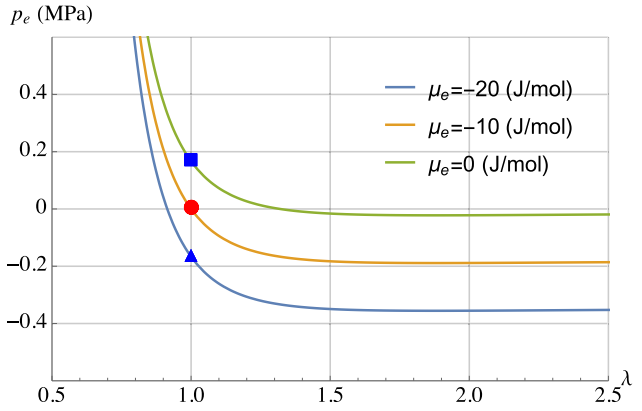

FIG. 2. Pressure–stroke curves $p_e(\lambda, \mu_e, \lambda_o)$ for three values of μ_e with $\lambda_o = 2$, corresponding to $\mu_o = -10$ J/mol. When $\mu_e < \mu_o$ ($\mu_e > \mu_o$) the corresponding blocking pressure is determined on the vertical axis $\lambda = 1$ in correspondence of the blue triangle (square) on the blue (green) curve.

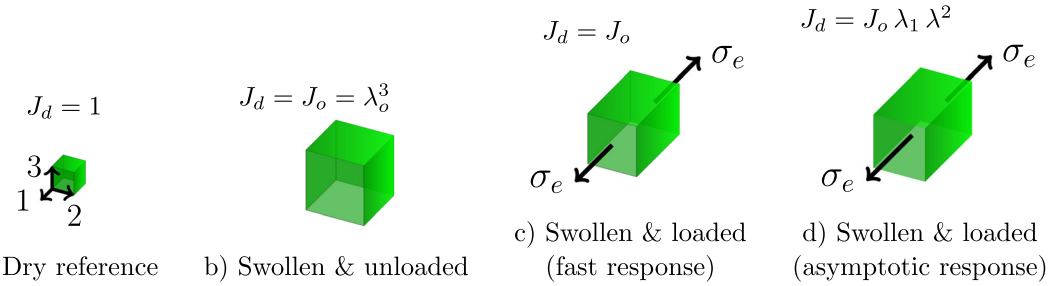

FIG. 3. From left to right: (a) dry state; (b) free-swollen state; (c) fast response state under swelling and loading; (d) asymptotic state under swelling and loading. For a gel with G = 0.1 MPa, $RT/\Omega = 40$ MPa, $\chi = 0.2$, under a traction $\sigma_e = 0.1$ MPa, we have: $J_o = 18.5$, $J_d \simeq 23$. Plots are in scale.

conditions, by uniaxial boundary loads σ_e per unit current area, and by a uniaxial step deformation λ_1. Both uniaxial loads and deformations induce a transversely isotropic deformation process

$$\mathbf{F} = \lambda_1 \mathbf{e}_1 \otimes \mathbf{e}_1 + \lambda \check{\mathbf{I}}, \quad \check{\mathbf{I}} = \mathbf{I} - \mathbf{e}_1 \otimes \mathbf{e}_1, \tag{2.23}$$

where it was assumed that loads and deformations are aligned with $\mathbf{e}_1$. The stress shares the transversely isotropic structure of the deformation $\mathbf{F}$ and is represented as $\mathbf{T} = \sigma_1 \mathbf{e}_1 \otimes \mathbf{e}_1 + \sigma \check{\mathbf{I}}$. From Equations $(2.3)_1$, $(2.4)_1$, (2.5), and $(2.12)_2$, we can write the constitutive equations of σ_1 and σ as

$$\sigma_1 = \frac{G}{\lambda^2 \lambda_o}\,\lambda_1 - p \quad \text{and} \quad \sigma = \frac{G}{\lambda_1 \lambda_o} - p. \tag{2.24}$$

The slow response of the gel is described by the steady solution of the stress–diffusion problem, under the following boundary conditions:

$$\mathbf{T}\mathbf{n} = \begin{cases} \sigma_e\,\mathbf{e}_1 & \text{for } \mathbf{n} = \mathbf{e}_1 \\ 0 & \text{for } \mathbf{n} = \mathbf{e}_2, \mathbf{e}_3 \end{cases} \quad \text{and} \quad \mu = \mu_e \quad \text{on } \partial\mathcal{B}_t\,.$$

Hence, the homogeneous solutions of the problem correspond to the mechanical and chemical balance equations, which prescribe that

$$\sigma_1 = \sigma_e,\ \sigma = 0, \quad \text{and} \quad \mu = \mu_e \quad \text{in } \mathcal{B}_t. \tag{2.25}$$

The chemical balance $(2.25)_3$, together with Equations $(2.3)_2$, yields the value attained by pressure p at the steady state

$$p = \frac{1}{\Omega}(\mu_e - \mu(J J_o)). \tag{2.26}$$

On the other hand, the mechanical balance $(2.25)_2$, together with Equation $(2.24)_2$, gives $p = G/\lambda_1\lambda_o$. Hence, using this latter into Equations $(2.25)_1$ together with Equation $(2.24)_1$ and into Equation (2.26) together with Equation (2.8), we get the two equations governing the steady response of the gel

$$\begin{aligned} &\frac{G}{\lambda_o}\left(\frac{\lambda_1}{\lambda^2} - \frac{1}{\lambda_1}\right) = \sigma_e, \\ &\mu(JJ_o) + \Omega\frac{G}{\lambda_o}\frac{1}{\lambda_1} = \mu_e, \quad J = \lambda_1\lambda^2\,. \end{aligned} \tag{2.27}$$

Equations (2.27) give the stretches λ_1 and λ, which define the shape of the gel parallelepiped $\mathcal{B}_t$ under the pair (σ_e, μ_e); alternatively, they characterize the normal boundary traction σ_e and the stretch λ under the pair (λ_1, μ_e).

This solution is shown in the λ_1–λ plane in Figure 4, where the brown–to–orange colours identify different values of μ_e (from −100 to 0 J/mol), whereas μ_o has been fixed as $\mu_o = -10$ J/mol. The red line is the iso–σ_1 (or equivalently, due to Equation (2.25), iso–σ_e) line corresponding to $\sigma_1 = 0$ kPa; the corresponding $\lambda_1 = \lambda$ values identify the size of the free–swelling states, at different values of μ_e. We can move from state 1 ($\lambda_1 = \lambda = 1$) to state 2 along the iso–μ_e line $\mu_e = -10$ J/mol, acting upon the gel with a traction $\sigma_e = 50$ kPa; then, from state 2 to state 3, keeping the traction fixed and increasing the chemical potential to a new value $\mu_e = 0$ J/mol; and from state 3 to state 4 along the new iso–μ_e line $\mu_e = 0$ J/mol removing the traction; and, at the end, go back to state 1 only changing μ_e to the old value $\mu_e = -10$ J/mol. The corresponding shapes of the cubic gel are shown, in scale, in the lateral panel in Figure 3.

Figure 4 also allows us to evaluate the traction σ_e corresponding to an imposed deformation λ_1 (which might represent the value prescribed by a boundary constraint), for different values of μ_e. As an example, for $\lambda_1 = 0.68$ we get $\sigma_e = -50$ kPa at $\mu_e = -10$ J/mol; it means that the freely swollen cube $\mathcal{B}_o$ with side length equal to λ_o, once

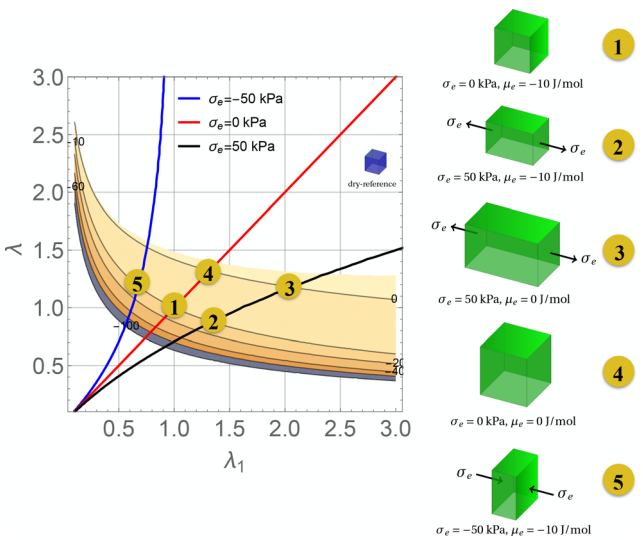

FIG. 4. Iso–traction lines $\sigma_1 = -50$ kPa (blue line), $\sigma_1 = 0$ kPa (red line), $\sigma_1 = 50$ kPa (black line) in the λ_1–λ plane over contour lines of μ_e (from −100 J/mol (brown) to 0 J/mol (light yellow). The state of the gel is pinpointed by the intersection of iso-traction lines with iso-potential lines: the circled numbers from 1 to 5 show five of such points on the line $\mu = -10$ J/mol (states 1, 2, and 5) and on the line $\mu = 0$ J/mol (states 3 and 4). On the right, the corresponding shapes of the gel are shown in scale.

constrained to reduce the length of the side aligned with $\mathbf{e}_1$ to $\lambda_1\lambda_o = 0.68\lambda_o$ would exert a traction equal to $-\sigma_e = 50\,\text{kPa}$ on the constraint.

A direct visualization of the blocking force $\sigma_r = -\sigma_e$, that is, of the traction exerted on the constraints hampering the deformation of the swollen state $\mathcal{B}_o$ along $\mathbf{e}_1$, is given in Figure 5: the blue square (triangle) on the green (blue) line identifies the traction acting on the constraint that maintains $\lambda_1 = 1$. It is worth noting that, being the gel isotropic, a completely equivalent situation would correspond to a constraint, which hampers the full deformation along the direction spanned by $\mathbf{e}_\alpha$, with $\alpha = 2, 3$. Our results are very similar to the ones in Ref. 13, where the same problem was discussed for isotropic temperature–sensitive hydrogels both from an experimental and theoretical point of view, through the so–called ideal elastomeric gel model.

For large swelling–induced deformations, i.e., $1/J_o \to 0$ and $1/J \to 0$, Equation (2.26) can be approximated as

$$p \simeq -\frac{RT}{\Omega}(\chi - 1/2)\frac{1}{J_o^2 J^2} \simeq \frac{G}{\lambda_o}\frac{1}{\lambda_1^2\lambda^4}, \tag{2.28}$$

where we used Equation (2.11) and set $\mu_o = \mu_e = 0$. With this, being $\sigma = 0$, we get the relationship which links the steady values λ_1 and λ (experimentally discussed in Ref. 14), as well as the asymptotic relationship valid at the steady state between σ_1 and λ_1

$$\lambda = \lambda_1^{-1/4} \quad \text{and} \quad \sigma_1 = \frac{G}{\lambda_o}\left(\lambda_1^{3/2} - \lambda_1^{-1}\right). \tag{2.29}$$

C. Fast response of isotropic gels

Figure 4 describes the asymptotic state under uniaxial step traction or deformation. It is also of interest to determine the mechanical state just after traction (or deformation) is applied and before diffusion starts; during such a transient, the gel behaves as an elastic and incompressible solid

$$J = 1 \quad \text{and} \quad \lambda = \lambda_1^{-1/2}; \tag{2.30}$$

moreover, its response is different. Indeed, from being $\sigma = 0$, we get the relationship holding between the before–diffusion–starts values σ_{1f} of the stress and λ_1

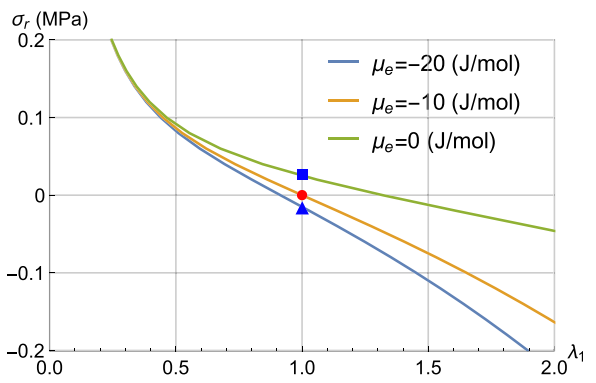

FIG. 5. Stress–stroke curves $\sigma_r = -\sigma_e(\lambda_1)$ at different values of μ_e when $\mu_o = -10\,\text{J/mol}$ and $\lambda_o = 2$, being $G = 0.1\,\text{MPa}$.

$$\sigma_{1f} = \frac{G}{\lambda_o}\left(\lambda_1^2 - \frac{1}{\lambda_1}\right), \tag{2.31}$$

where the Equation $(2.30)_2$ has been taken into account.

A comparison between Equations (2.29) and (2.31) allows us to identify both the force relaxation due to a step deformation and the creep due to diffusion in response to a step load, a phenomenon which is different from the one characteristic of the viscoelastic response of solids, as discussed in Ref. 14.

III. ANISOTROPIC GELS UNDER UNIAXIAL TRACTION AND EXTENSION

For anisotropic gels, we proposed in Ref. 6 an extension of the classical Flory–Rehner model, where the elastic term ψ_e in the free energy ψ has the following form:

$$\psi_e(\mathbf{F}_d) = \frac{G}{2}(\mathbf{F}_d \cdot \mathbf{F}_d - 3) + \frac{1}{2}G\gamma\,(\mathbf{F}_d\,\mathbf{e}\cdot\mathbf{F}_d\,\mathbf{e} - 1)^2, \tag{3.1}$$

where γ is a stiffening parameter, and the unit vector $\mathbf{e}$ describes the fibers' direction. Behind the representation (3.1), there is the idea to describe the effect of the presence of reinforcements (fibers) into the gel, which hampers the swelling along their direction. Within that context, the dry–reference stress $\mathbf{S}_d$ is represented by Equation $(2.3)_1$ with

$$\mathbf{S}_d(\mathbf{F}_d) = G\,\mathbf{F}_d + 2\,G\,\gamma\,(\mathbf{C}_d \cdot \mathbf{E} - 1)\mathbf{F}_d\,\mathbf{E}, \tag{3.2}$$

being $\mathbf{C}_d = \mathbf{F}_d^T\mathbf{F}_d$ the right Cauchy-Green strain, and $\mathbf{E} = \mathbf{e}\otimes\mathbf{e}$ the direction of the fiber $\mathbf{e}$. We are interested in homogeneous solutions of the swelling problem, which realize the following triaxial deformation $\mathbf{F}_d$:

$$\mathbf{F}_d = \lambda_{di}\mathbf{E}_i, \quad \mathbf{E}_i = \mathbf{e}_i \otimes \mathbf{e}_i,\ i = 1, 2, 3, \tag{3.3}$$

compatible with fibres aligned with $\mathbf{e}_1$ or $\mathbf{e}_2$ or $\mathbf{e}_3$. The (Cauchy) stress $\mathbf{T}$ admits the following representation

$$\mathbf{T} = \frac{1}{J_d}\,G\left(\mathbf{B}_d + 2\,\gamma\,(\mathbf{C}_d \cdot \mathbf{E} - 1)\mathbf{F}_d\,\mathbf{E}\,\mathbf{F}_d^T\right) - p\,\mathbf{I}, \tag{3.4}$$

being, in this case, $\mathbf{B}_d = \mathbf{C}_d = \lambda_{di}^2\,\mathbf{E}_i$. Given a plane in the dry-reference configuration having unit normal $\mathbf{m}$, the image under $\mathbf{F}_d$ of that plane will have a normal $\mathbf{n}$ represented by

$$\mathbf{n} = \frac{\mathbf{F}_d^\star\,\mathbf{m}}{|\mathbf{F}_d^\star\,\mathbf{m}|} = \frac{\lambda_i^{-1}\,\mathbf{E}_i\,\mathbf{m}}{|\lambda_i^{-1}\,\mathbf{E}_i\,\mathbf{m}|}; \tag{3.5}$$

Denoting with $\mathbf{t}$ a unit vector orthogonal to $\mathbf{n}$, the normal and tangential stress component of $\mathbf{T}$ with respect to $\mathbf{n}$ and $\mathbf{t}$ are $\sigma_\mathbf{n} = \mathbf{T}\,\mathbf{n}\cdot\mathbf{n}$ and $\tau_\mathbf{n} = \mathbf{T}\,\mathbf{n}\cdot\mathbf{t}$, and are given by

$$\begin{aligned}
\sigma_\mathbf{n} &= \frac{G}{J_d}\,\lambda_{di}^2\,(\mathbf{n}\cdot\mathbf{e}_i)^2 - p \\
&\quad + 2\,\frac{G\,\gamma}{J_d}\left(\lambda_{di}^2\,(\mathbf{e}\cdot\mathbf{e}_i)^2 - 1\right)\left(\lambda_{di}\,(\mathbf{n}\cdot\mathbf{e}_i)\,(\mathbf{e}\cdot\mathbf{e}_i)\right)^2, \\
\tau_\mathbf{n} &= \frac{G}{J_d}\,\lambda_{di}^2\,(\mathbf{n}\cdot\mathbf{e}_i)\,(\mathbf{t}\cdot\mathbf{e}_i) + 2\,\frac{G\,\gamma}{J_d}\left(\lambda_{di}^2\,(\mathbf{e}\cdot\mathbf{e}_i)^2 - 1\right) \\
&\quad \times \left(\lambda_{di}\,(\mathbf{n}\cdot\mathbf{e}_i)\,(\mathbf{e}\cdot\mathbf{e}_i)\right)\left(\lambda_{di}\,(\mathbf{t}\cdot\mathbf{e}_i)\,(\mathbf{e}\cdot\mathbf{e}_i)\right).
\end{aligned} \tag{3.6}$$

For anisotropic gels, free–swelling states yield changes in both size and shape.[5] As for the isotropic gel, balance laws prescribe $\mathbf{S}_d = \mathbf{0}$ and $\mu_e = \mu_o$; the free-swollen state $\mathcal{B}_o$, deformed by $\mathbf{F}_d = \mathbf{F}_o = \lambda_{o\|}\,\mathbf{E} + \lambda_{o\perp}\hat{\mathbf{I}}$ with respect to $\mathcal{B}_d$, is completely defined by the value μ_o of the bath's chemical potential. Let us only note that, for $\mu_o = 0$, the relationship between $\lambda_{o\|}$ and $\lambda_{o\perp}$ prescribes that

$$\lambda_{o\perp}^2 = \lambda_{o\|}^2(1 + 2\gamma(\lambda_{o\|}^2 - 1)), \tag{3.7}$$

and for large deformation ($1/J_o \to 0$), it holds

$$\frac{RT}{\Omega}(\chi - 1/2)\frac{1}{J_o^2} = -\frac{G}{\lambda_{o\|}}, \quad J_o = \lambda_{\|}\lambda_{\perp}^2. \tag{3.8}$$

In the following, we present and discuss the slow and fast responses of anisotropic gels to imposed uniaxial tractions and/or deformations, with reference to a unit cube $\mathcal{B}_d$ at dry state, having fibers aligned along the direction $\mathbf{e} = \mathbf{e}_1$ (panel (a) in Figure 6), which realizes a free–swollen state $\mathcal{B}_o$ with a bath's chemical potential equal to μ_o (panel (b) in Figure 6). The free-swollen gel may experience a further deformation determined by a change of the bath's potential, by the action of uniaxial boundary loads σ_e per unit current area, or by a uniaxial step extension.

We shall examine two cases: (A) corresponds to normal boundary tractions on the faces of unit normal $\pm\mathbf{e}_1$ or, equivalently, to impose a deformation λ_1 (Section III A); (B) corresponds to normal boundary tractions on the faces of unit normal $\pm\mathbf{e}_2$ or, equivalently, to impose a stretch of intensity λ_2 along $\mathbf{e}_2$ (Section III B).

A. Parallel–to–the–fibers normal loads

The deformation is transversely isotropic; thus, $\lambda_{d1} = \lambda_{d\|}$, and $\lambda_{d2} = \lambda_{d3} = \lambda_{d\perp}$, being $\lambda_{d\|}$ and $\lambda_{d\perp}$ the linear swelling ratios along the fiber direction $\mathbf{E} = \mathbf{E}_1$ and in the orthogonal plane $\check{\mathbf{I}} = \mathbf{I} - \mathbf{E} = \mathbf{E}_2 + \mathbf{E}_3$, respectively

$$\mathbf{F}_d = \lambda_{d\|}\mathbf{E} + \lambda_{d\perp}\check{\mathbf{I}}. \tag{3.9}$$

We can set the stress–diffusion problem in the dry state $\mathcal{B}_d$ and look for homogeneous steady solutions which are driven by the boundary conditions

$$\mathbf{S}_d\mathbf{m} = \begin{cases} s_e\mathbf{e}_1 & \text{for } \mathbf{m} = \mathbf{e}_1, \\ 0 & \text{for } \mathbf{m} = \mathbf{e}_2, \mathbf{e}_3, \end{cases} \quad \text{and} \quad \mu = \mu_e,$$

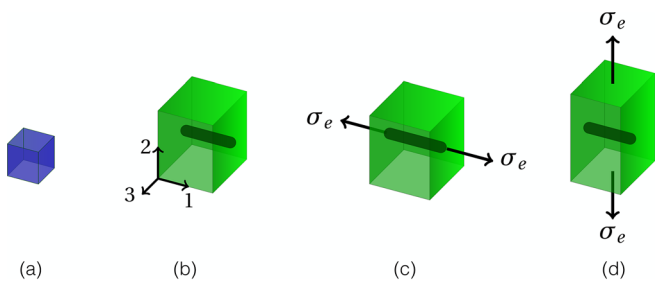

FIG. 6. From left to right: (a) dry state; (b) free–swollen state: $\sigma_e = 0$, and $\mu_e = -10$ J/mol; (c) swollen with traction along the fiber: $\sigma_e = 50$ kPa, and $\mu_e = -10$ J/mol; (d) swollen with traction orthogonal to the fiber: $\sigma_e = 50$ kPa, and $\mu_e = -10$ J/mol.

on $\partial\mathcal{B}_d$, being $s_e = \lambda_{d\perp}^2\sigma_e$ the uniaxial and normal boundary load per unit dry area, and σ_e the corresponding load per unit of current area (see panel (c) in Figure 6). Hence, mechanical and chemical balances prescribe

$$s_{d\|} = s_e, \quad s_{d\perp} = 0, \quad \text{and} \quad \mu = \mu_e \quad \text{in } \mathcal{B}_d, \tag{3.10}$$

being $\mathbf{S}_d = s_{d\|}\mathbf{E} + s_{d\perp}\check{\mathbf{I}}$ the representation of the dry–reference stress. The anisotropy of the gel is of elastic nature and does not change the constitutive structure of the chemical potential; hence, the chemical balance $(3.10)_3$, together with Equations $(2.3)_2$, yields the osmotic pressure field in the form given by Equation (2.26). Once used this last equation together with (3.2) into $(2.3)_1$, the mechanical balance $(3.10)_2$ yields

$$\mu(J_d) + \frac{\Omega G}{\lambda_{d\|}} = \mu_e, \quad J_d = \lambda_{d\|}\,\lambda_{d\perp}^2; \tag{3.11}$$

this last relation characterizes $\lambda_{d\perp}$ in terms of μ_e and $\lambda_{d\|}$: $\lambda_{d\perp} = \lambda_{d\perp}(\lambda_{d\|}, \mu_e)$. Equations (2.26), (3.2), and $(2.3)_1$ allow us to evaluate the stress component $s_{d\|}$. Being $s_{d\|} = s_e = \lambda_{d\perp}^2\sigma_e$, we get

$$\sigma_e = \frac{G\,\lambda_{d\|}}{\lambda_{d\perp}^2}\left(1 + 2\,\gamma\left(\lambda_{d\|}^2 - 1\right)\right) - \frac{G}{\lambda_{d\|}}. \tag{3.12}$$

Equation (3.12) also delivers $\sigma_{\mathbf{e}_1}$, being this latter equal to σ_e; from Equation (3.6), we get as expected $\tau_{\mathbf{e}_1} = 0$, i.e., no tangential tractions are exerted on the face of unit normal $\mathbf{e}_1$.

Equations (3.11) and (3.12) determine $\lambda_{d\|}$ and $\lambda_{d\perp}$ in terms of the pair (σ_e, μ_e), when these latter are the control parameters of the deformation process or, equivalently, allow us to evaluate $\lambda_{d\perp}$ and σ_e in terms of the pair $(\lambda_{\|}, \mu_e)$ when a deformation $\lambda_{\|} = \lambda_{d\|}/\lambda_{o\|}$ is imposed on the free–swollen state $\mathcal{B}_o$.

The solution is shown in the $\lambda_{d\|} - \lambda_{d\perp}$ plane in Figure 7 for $G = 0.1$ MPa and $\gamma = 0.1$, where we used the same color code as in Figure 4 for μ_e, ranging from -100 J/mol (brown) to 0 J/mol (light yellow). The red line is the iso–σ_e line corresponding to $\sigma_e = 0$, which is no longer along the bisectrix of the plane due to the anisotropic swelling: $\lambda_{d\|}$ is always smaller than $\lambda_{d\perp}$.

The corresponding $\lambda_{d\|}$ and $\lambda_{d\perp}$ values identify the size of the free–swelling states, at different values of μ_e. We can move from state 1 ($\lambda_{d\|} = 1.77$ and $\lambda_{d\perp} = 2.12$) to state 2 along the iso-potential line $\mu_e = -10$ J/mol, acting upon the gel with a traction $\sigma_e = 50$ kPa; then, from 2 to 3, along the iso-traction line $\sigma_e = 50$ kPa, by increasing the chemical potential to the new value $\mu_e = 0$ J/mol; from 3 to 4 along the new iso-potential line $\mu_e = 0$ J/mol, and removing the traction; then, eventually, go back to state 1 by decreasing μ_e to the initial value $\mu_e = -10$ J/mol. The corresponding actual shapes realized by the gel cube are shown, in scale, in the lateral panel in Figure 7.

We may compare asymptotic and fast response of isotropic gels under uniaxial traction with the corresponding responses of anisotropic gels under uniaxial traction aligned with fiber direction. For large swelling–induced deformations, i.e., $1/J_o \to 0$ and $1/J \to 0$, Equation (2.26) can be approximated as

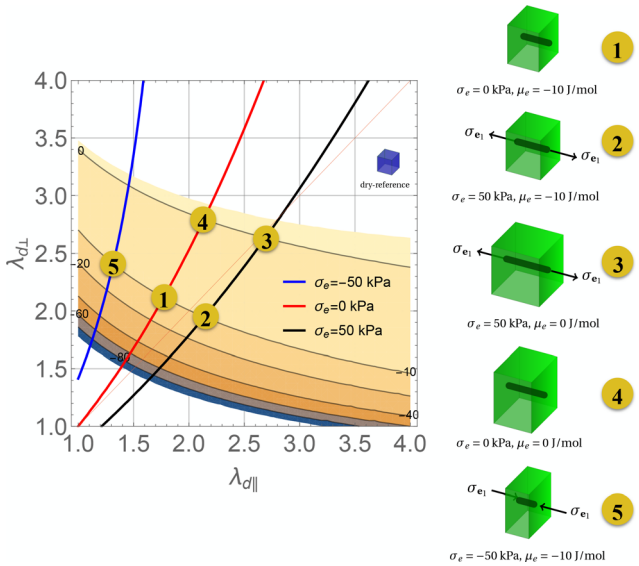

FIG. 7. Iso–traction lines $\sigma_e = -50$ kPa (blue line), $\sigma_e = 0$ kPa (red line), $\sigma_e = 50$ kPa (black line) in the $\lambda_{d1}-\lambda_{d2}$ plane, over contour lines of μ_e (from -100 J/mol (brown) to 0 J/mol (light yellow). The state of the gel is pinpointed by the intersection of iso-traction lines with iso-potential lines: the circled numbers from 1 to 5 show five of such points on the line $\mu = -10$ J/mol (states 1, 2, and 5) and on the line $\mu = 0$ J/mol (states 3 and 4). On the right, the corresponding shapes of the gel are shown in scale.

$$p \simeq -\frac{RT}{\Omega}(\chi - 1/2)\frac{1}{J_o^2 J^2} \simeq \frac{G}{\lambda_{o\parallel}}\frac{1}{J^2}, \tag{3.13}$$

where we set $\mu_o = \mu_e = 0$. Under the asymptotic approximation determined by the Equation (3.13), mechanical balance $(3.10)_{1,2}$ yields $\lambda_\perp = \lambda_\parallel^{-1/4}$ and $\sigma_{\mathbf{e}_1} = \sigma_e$ as

$$\sigma_{\mathbf{e}_1} = \frac{G}{\lambda_{o\parallel}}\left(\alpha(\lambda_\parallel, \gamma)\,\lambda_\parallel^{3/2} - \lambda_\parallel^{-1}\right), \tag{3.14}$$

with

$$\alpha(\lambda_\parallel, \gamma) = \frac{1 + 2\gamma\left(\lambda_{o\parallel}^2\,\lambda_\parallel^2 - 1\right)}{1 + 2\gamma\left(\lambda_{o\parallel}^2 - 1\right)}. \tag{3.15}$$

The relationship between the two stretches is the same as in the isotropic case and says that Poisson modulus at the steady state is 1/4; on the other hand, as $\alpha(\lambda_\parallel, 0) = 1$, for $\gamma = 0$ Equation (3.14) delivers Equation $(2.29)_2$ and the isotropic case is recovered.

The fast response to the deformation $\lambda_\parallel$ is driven by the anisotropic elastic nature of the network. Before diffusion starts, we have $J = \lambda_\parallel \lambda_\perp^2 = 1$; Equations $(3.10)_{1,2}$ yield the pressure field p and

$$\sigma_{f\mathbf{e}_1} = \frac{G}{\lambda_{o\parallel}}\left(\alpha(\lambda_\parallel, \gamma)\,\lambda_\parallel^2 - \lambda_\parallel^{-1}\right). \tag{3.16}$$

The difference between the two stresses is a measure of the swelling–induced relaxation in the gel. Figure 8 shows the differences in stress relaxation due to the anisotropy when $\gamma = 1$. Comparing isotropic and anisotropic response curves, it can be noted that anisotropy enhances stress relaxation when the imposed uniaxial deformation is aligned with fiber direction.

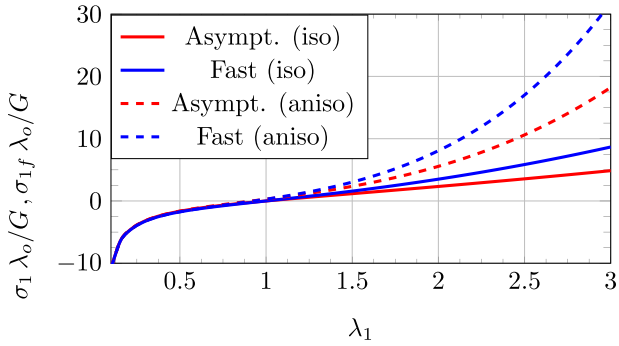

FIG. 8. The swelling–induced stress reduction in isotropic gels is measured by the difference between the blue solid line (Equation (2.31)) and the red solid line (Equation (2.29)) at the same value of the imposed deformation λ_1. That difference represents material relaxation due to diffusion. The corresponding dashed lines measure the swelling–induced stress reduction in the presence of fibers ($\gamma = 1$ and $\lambda_{o\parallel} = 2$) as difference between the blue dashed line (Equation (3.16)) and the red dashed line (Equation (3.14)) at the same value of the imposed deformation $\lambda_1 = \lambda_\parallel$.

B. Transverse–to–the–fibers normal loads

In this case, fibres and tractions are not aligned and the deformation $\mathbf{F}_d$ maintains the triaxial anisotropic structure given by (3.3). We look for homogeneous solutions of the stress–diffusion problem posed on the dry configuration $\mathcal{B}_d$, under the following boundary conditions

$$\mathbf{S}_d\,\mathbf{m} = \begin{cases} \mathbf{0} & \text{for } \mathbf{m} = \mathbf{e}_1, \mathbf{e}_3, \\ s_e\,\mathbf{e}_2 & \text{for } \mathbf{m} = \mathbf{e}_2, \end{cases} \quad \text{and} \quad \mu = \mu_e$$

on $\partial\mathcal{B}_d$. Hence, mechanical and chemical balances prescribe

$$s_{d1} = s_{d3} = 0,\ s_{d2} = s_e, \quad \text{and} \quad \mu = \mu_e \text{ in } \mathcal{B}_d, \tag{3.17}$$

being $\mathbf{S}_d = s_{di}\mathbf{e}_i \otimes \mathbf{e}_i$, $(i = 1, 2, 3)$, the appropriate representation of the dry–reference stress. The anisotropy of the gel is of elastic nature and does not change the constitutive formula of the chemical potential; hence, the chemical balance $(3.17)_3$, together with Equations $(2.3)_2$, yield the osmotic pressure field in the form given by the Equation (2.26). Once used this last equation into $(2.3)_1$ and (3.2), the mechanical balance $(3.17)_2$ yields

$$\mu(J_d) + \frac{\Omega G}{\lambda_{d1}\,\lambda_{d2}}\,\lambda_{d3} = \mu_e, \quad J_d = \lambda_{d1}\,\lambda_{d2}\,\lambda_{d3}. \tag{3.18}$$

On the other hand, Equation $(3.17)_1$ delivers

$$\lambda_{d3}^2 = (1 + 2\gamma\,(\lambda_{d1}^2 - 1))\,\lambda_{d1}^2, \tag{3.19}$$

that is, yields the relation $\lambda_{d3} = \lambda_{d3}(\lambda_{d1})$. Equations (3.18) and (3.19) concoct the representation of λ_{d1} in terms of λ_{d2} and μ_e: $\lambda_{d1} = \lambda_{d1}(\lambda_{d2}, \mu_e)$. Equations (2.26), (3.2), and $(2.3)_1$ allow us to evaluate the stress component s_{d2}. Being $s_{d2} = s_e = \lambda_{d1}\,\lambda_{d3}\,\sigma_e$, we get

$$\sigma_e = \frac{G}{\lambda_{d1}}\left(\frac{\lambda_{d2}}{\lambda_{d3}} - \frac{\lambda_{d3}}{\lambda_{d2}}\right), \tag{3.20}$$

with $\lambda_{d3} = \lambda_{d3}(\lambda_{d1})$ and $\lambda_{d1} = \lambda_{d1}(\lambda_{d2}, \mu_e)$.

Equation (3.20) also delivers $\sigma_{\mathbf{e}_2}$, as $\sigma_{\mathbf{e}_2} = \sigma_e$; from Equation $(3.6)_2$, we get as expected $\tau_{\mathbf{e}_2} = 0$, i.e., no tangential tractions are exerted on the face of unit normal $\mathbf{e}_2$ under this deformation process.

C. Blocking forces

The characterisation of stroke curves in the anisotropic gel actuator is especially interesting as both normal and tangential blocking forces can arise, depending on the anisotropic structure of the gel.

In the case parallel–to–the–fibers normal blocking forces, and with reference to Section III A, σ_e may be viewed as the boundary traction exerted on the body by constraints hampering deformation along $\mathbf{e}_1$ (see inset (a) in Figure 9). In this case, Figure 9 shows, for different values of μ_e, the traction corresponding to the constraints which prescribes a stretch intensity $\lambda_{d\|} = \lambda_c$. Precisely, by using Equation (3.11) to characterize the relation $\lambda_{d\perp} = \lambda_{d\perp}(\lambda_{d\|}, \mu_e)$, it can be derived from (3.12) the family of stroke curves $\sigma_r = -\sigma_e(\lambda_{d\|}, \mu_e)$ which is shown in Figure 9 (solid lines, with $\lambda_c = \lambda_{d\|}$). The intercepts of the curves with the vertical axis $\lambda_c = 1$ yield the corresponding blocking forces

$$\sigma_r = -\sigma_e(1, \mu_e) = -G\left(\frac{1}{\lambda_{d\perp}^2} - 1\right), \tag{3.21}$$

being $\lambda_{d\perp} = \lambda_{d\perp}(1, \mu_e)$. Equation (3.21) shows that $\sigma_r = 0$ for $\lambda_{d\perp} = 1$; however, from being $\lambda_{d\perp} = \lambda_{d\perp}(1, \mu_e)$, it occurs that $\lambda_{d\perp} = 1$ if $\mu_e \to -\infty$. Hence, when constraints maintain the gel in the dry configuration under the special bath conditions characterised by $\mu_e \to -\infty$, blocking forces are null as that configuration is stress–free.

Due to the anisotropic response, the characteristic stroke curves are different when transverse–to–the–fibers–normal loads are considered. We view σ_e as the boundary traction exerted on the body by constraints hampering deformation along $\mathbf{e}_2$ (see the right inset in Figure 9), and evaluate, for different values of μ_e, the traction corresponding to a prescribed stretch $\lambda_{d2} = \lambda_c$. Precisely, using Equation (3.19) to characterise λ_{d3} as $\lambda_{d3}(\lambda_{d1})$ and Equation (3.18) to characterise λ_{d1} as $\lambda_{d1}(\lambda_{d2}, \mu_e)$, the family of stroke curves $\sigma_r = -\sigma_e(\lambda_{d2})$ for different values of μ_e are shown in Figure 9 (dashed lines, with $\lambda_c = \lambda_{d2}$). The intercepts of the stroke curves with the vertical axis $\lambda_c = 1$ define the blocking forces for different μ_e

$$\sigma_r = -\sigma_{\mathbf{e}_2} = \frac{G}{\lambda_{d1}}\left(\frac{1}{\lambda_{d3}} - \lambda_{d3}\right), \tag{3.22}$$

with $\lambda_{d3} = \lambda_{d3}(\lambda_{d1})$, and $\lambda_{d1} = \lambda_{d1}(1, \mu_e)$. In contrast to what happens in isotropic gels, stroke–curves (dashed lines) are different from the ones discussed in the Section III A (solid lines), and the blocking forces exerted on the orthogonal faces of unit normals $\mathbf{e}_1$ and $\mathbf{e}_2$ are not the same, as Figure 9 evidences (look at the intercepts of the stroke curves with the vertical axis $\lambda_c = 1$).

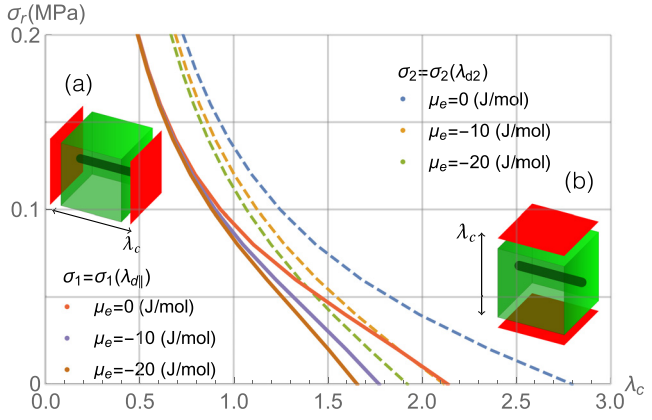

FIG. 9. Stroke curves $\sigma_r(\lambda_c)$ for different values of μ_e: case a) $-\sigma_1(\lambda_{d\|})$ (solid lines); case b) $-\sigma_2(\lambda_{d2})$ (dashed lines). The insets show the constraints (red surfaces) acting on the fibered gel cube in the two cases (a) (left) and (b) (right).

IV. ANISOTROPIC GELS UNDER TANGENTIAL FORCES

Interestingly, the range of blocking forces generated by an anisotropic gel is quite large, as free–swelling can also induce shear, depending on the anisotropy directions.

Let us consider a fiber distribution within the hydrogel aligned along $\mathbf{e} = \sqrt{2}/2\mathbf{e}_1 + \sqrt{2}/2\mathbf{e}_2$, a situation that can be easily generalized. We imagine that appropriate constraints hamper the swelling in both the directions $\mathbf{m} = \mathbf{e}_1$ and $\mathbf{m} = \mathbf{e}_2$, so allowing the initial dry unit cube to swell into a parallelepiped of side λ_{d1} and λ_{d2}, having in general $\lambda_{d1} \neq \lambda_{d2}$, and both of them smaller than $\lambda_{f\|}$, that is, the linear swelling ratio along fiber's direction corresponding under a chemical potential μ_e to free swelling conditions (see Figure 10). Hence, we assume that the representation (3.3) of $\mathbf{F}_d$ still holds. We look for homogeneous solutions of the stress–diffusion problem posed on the dry configuration $\mathcal{B}_d$, under the boundary conditions

$$\mathbf{S}_d\,\mathbf{m} = \mathbf{0} \text{ for } \mathbf{m} = \mathbf{e}_3 \quad \text{and} \quad \mu = \mu_e \quad \text{on } \partial\mathcal{B}_d, \tag{4.1}$$

and prescribed values of λ_{d1} and λ_{d2}. Hence, mechanical and chemical balances prescribe

$$s_{d3} = 0 \quad \text{and} \quad \mu = \mu_e \quad \text{in } \mathcal{B}_d, \tag{4.2}$$

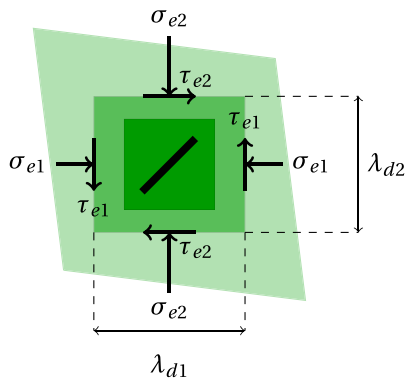

FIG. 10. Sketch of the plane section of unit normal $\mathbf{e}_3$ of the unit cube at the dry state (dark green square), at the free–swelling state (light green diamond), and at the constrained state (green rectangle).

that is, using Equations (3.2) and (4.1),

$$p = G\,\frac{\lambda_{d3}}{\lambda_{d1}\lambda_{d2}},$$
$$\mu(J_d) + \Omega\, G\,\frac{\lambda_{d3}}{\lambda_{d1}\lambda_{d2}} = \mu_e, \quad J_d = \lambda_{d1}\lambda_{d2}\lambda_{d3}. \tag{4.3}$$

Equation $(4.3)_2$ implicitly characterizes λ_{d3} in terms of μ_e and the pair $(\lambda_{d1}, \lambda_{d2})$, here considered as parameters.

We consider the traction on the face of unit normal $\mathbf{m} = \mathbf{e}_1$; we have $\mathbf{n} = \mathbf{e}_1$ and fix $\mathbf{t} = \mathbf{e}_2$. With this, Equations (3.6) prescribe

$$\sigma_{\mathbf{e}_1} = G\left(\frac{\lambda_{d1}}{\lambda_{d2}\,\lambda_{d3}}\left(1 + \gamma\left(\frac{\lambda_{d1}^2 + \lambda_{d2}^2}{2} - 1\right)\right) - \frac{\lambda_{d3}}{\lambda_{d1}\,\lambda_{d2}}\right),$$
$$\tau_{\mathbf{e}_1} = G\,\gamma\,\frac{1}{\lambda_{d3}}\left(\frac{\lambda_{d1}^2 + \lambda_{d2}^2}{2} - 1\right). \tag{4.4}$$

Due to the symmetry of the stress, tangential traction $\tau_{\mathbf{e}_2}$ on the face of unit normal $\mathbf{m} = \mathbf{e}_2$ (that is, for $\mathbf{n} = \mathbf{e}_2$) is equal to $\tau_{\mathbf{e}_1}$, whereas in general $\sigma_{\mathbf{e}_1} \neq \sigma_{\mathbf{e}_2}$. Using Equations $(4.3)_2$ and (4.4), we can evaluate the normal stroke curves of the gel as $\sigma_r(\lambda_{d1})$ at $\lambda_{d2} = 1$ and $\sigma_r(\lambda_{d2})$ at $\lambda_{d1} = 1$, at different values of the solvent bath's potential μ_e. Likewise, we can evaluate the tangential stroke curves $\tau_r(\lambda_{d2})$ at $\lambda_{d1} = 1$. It is worth noting that for $\lambda_{d1} = \lambda_{d2} = 1$, it holds

$$\sigma_{\mathbf{e}_1} = \sigma_{\mathbf{e}_2} = G\left(\frac{1}{\lambda_{d3}} - \lambda_{d3}\right), \tag{4.5}$$

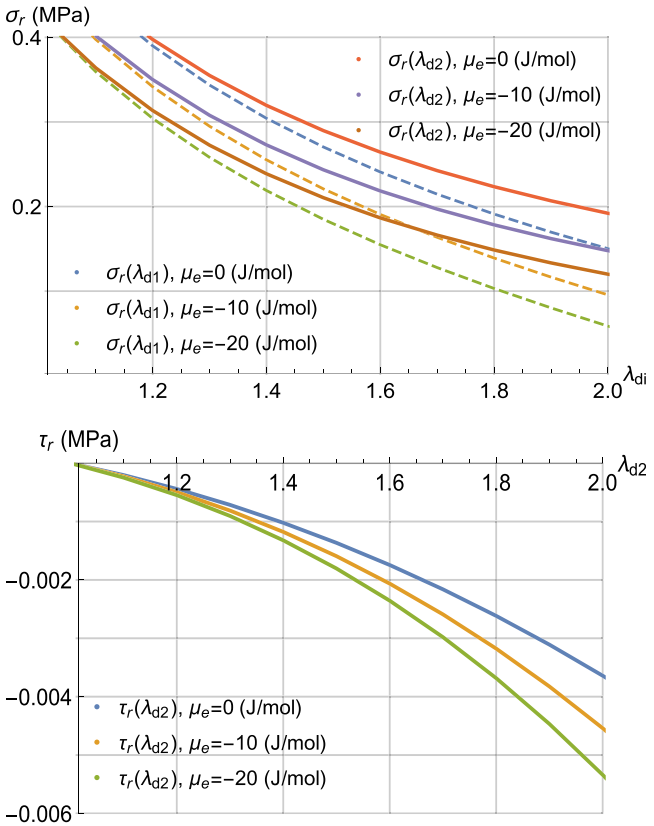

FIG. 11. Normal stroke curves $\sigma_r(\lambda_{d1})$ at $\lambda_{d2} = 1$ and $\sigma_r(\lambda_{d2})$ at $\lambda_{d1} = 1$ and tangential stroke curves $\tau_r(\lambda_{d2})$ at $\lambda_{d1} = 1$ at different values of μ_e, being $G = 0.1$ MPa and $\gamma = 0.1$.

and $\tau_{\mathbf{e}_1} = \tau_{\mathbf{e}_2} = 0$. Figure 11 shows normal and tangential stroke curves corresponding to $G = 0.1$ MPa, $\gamma = 0.1$, and for different values of μ_e; the range of λ_{d2} goes from 1, corresponding to dry conditions (being also $\lambda_{d1} = 1$), to $\lambda_{d\|}$ (which is around 2.1 with the aforementioned values of G and γ). Normal blocking forces are always positive, and tangential blocking forces are always negative, according to the cartoon shown in Figure 10.

V. CONCLUSIONS

We investigated performances of anisotropic gels driven by mechanical and chemical stimuli, in terms of both deformation processes and stroke–curves. In some cases, we distinguished between the fast response of gels before-diffusion-starts, and the asymptotic response attained at the steady state, highlighting the difference in material relaxation due to diffusion.

We also showed as anisotropic gel–based actuators can exert tangential, other than normal, blocking forces when fibers and constraints are not parallel and/or orthogonal each other. This kind of performance may be useful in actuator applications, which have not been extensively studied when fibrous hydrogels are involved, even if literature concerning technological applications is increasing.

ACKNOWLEDGMENTS

L.T. acknowledges the National Group of Mathematical Physics (GNFM–INdAM) for support.

[1]S. Dai, P. Ravi, and K. C. Tam, "Thermo- and photo-responsive polymeric systems," Soft Matter **5**, 2513–2533 (2009).
[2]J. Kim, J. A. Hanna, R. C. Hayward, and C. D. Santangelo, "Thermally responsive rolling of thin gel strips with discrete variations in swelling," Soft Matter **8**, 2375–2381 (2012).
[3]P. Nardinocchi and M. Pezzulla, "Curled actuated shapes of ionic polymer metal composites strips," J. Appl. Phys. **113**, 224906 (2013).
[4]M. Pezzulla, S. A. Shillig, P. Nardinocchi, and D. P. Holmes, "Morphing of geometric composites via residual swelling," Soft Matter **11**, 5812–5820 (2015).
[5]P. Nardinocchi, M. Pezzulla, and L. Teresi, "Steady and transient analysis of anisotropic swelling in fibered gels," J. Appl. Phys. **118**, 244904 (2015).
[6]P. Nardinocchi, M. Pezzulla, and L. Teresi, "Anisotropic swelling of thin gel sheets," Soft Matter **11**, 1492–1499 (2015).
[7]A. Osorio-Madrazo, M. Eder, M. Rueggeberg, J. K. Pandey, M. J. Harrington, Y. Nishiyama, J.-L. Putaux, C. Rochas, and I. Burgert, "Reorientation of cellulose nanowhiskers in agarose hydrogels under tensile loading," Biomacromolecules **13**, 850–856 (2012), pMID: 22295902.
[8]Y. Liu, X. Yong, G. McFarlin, O. Kuksenok, J. Aizenberg, and A. C. Balazs, "Designing a gel-fiber composite to extract nanoparticles from solution," Soft Matter **11**, 8692–8700 (2015).
[9]L. E. Millon and W. K. Wan, "The polyvinyl alcohol-bacterial cellulose system as a new nanocomposite for biomedical applications," J. Biomed. Mater. Res. Part B: Appl. Biomater. **79B**, 245–253 (2006).
[10]N. Miyamoto, M. Shintate, S. Ikeda, Y. Hoshida, Y. Yamauchi, R. Motokawa, and M. Annaka, "Liquid crystalline inorganic nanosheets for facile synthesis of polymer hydrogels with anisotropies in structure, optical property, swelling/deswelling, and ion transport/fixation," Chem. Commun. **49**, 1082–1084 (2013).
[11]Y. Liu, H. Zhang, J. Zhang, and Y. Zheng, "Constitutive modeling for polymer hydrogels: A new perspective and applications to anisotropic hydrogels in free swelling," Eur. J. Mech. A **54**, 171 (2015).
[12]S. Cai, Y. Lou, P. Ganguly, A. Robisson, and Z. Suo, "Force generated by a swelling elastomer subject to constraint," J. Appl. Phys. **107**, 103535 (2010).

[13]W. R. K. Illeperuma, J.-Y. Sun, Z. Suo, and J. J. Vlassak, "Force and stroke of a hydrogel actuator," Soft Matter **9**, 8504–8511 (2013).
[14]K. Urayama and T. Takigawa, "Volume of polymer gels coupled to deformation," Soft Matter **8**, 8017–8029 (2012).
[15]A. Lucantonio, P. Nardinocchi, and L. Teresi, "Transient analysis of swelling-induced large deformations in polymer gels," J. Mechan. Phys. Solids **61**, 205–218 (2013).
[16]P. J. Flory and J. Rehner, "Statistical mechanics of cross-linked polymer networks I. Rubberlike elasticity," J. Chem. Phys. **11**, 512–520 (1943).
[17]P. J. Flory and J. Rehner, "Statistical mechanics of cross-linked polymer networks II. Swelling," J. Chem. Phys. **11**, 521–526 (1943).
[18]We note that by considering the atmospheric pressure p_a acting on $\mathcal{B}_o$, a correction factor must be added to the potential μ_o: Equation (2.10) rewrites as $\mu(J_o) + \frac{G}{\lambda_o}\Omega = \mu_o - p_a\Omega$; being $\Omega \simeq 10^{-5}$ m^3/mol and $p_a \simeq 10^5$ Pa, the extra term to be added to μ_o is $p_a\,\Omega \simeq 1$ J/mol.
[19]Known both G and Ω, an experimental setting with μ_o as control parameter allows to measure λ_o and, from (2.11), the Flory parameter χ.[14]